NEPHELINE-RICH FOIDOLITES AND RARE-EARTH MINERALIZATION IN THE EL PICACHO TERTIARY INTRUSIVE COMPLEX, SIERRA DE TAMAULIPAS, NORTHEASTERN MEXICO

MARIANO ELÍAS-HERRERA, RAÚL RUBINOVICH-KOGAN, RUFINO LOZANO-SANTA CRUZ AND JOSÉ LUIS SÁNCHEZ-ZAVALA

Instituto de Geología, Universidad Nacional Autónoma de México, Ciudad Universitaria, Delegación Coyoacán, 04510 México, D.F., México

ABSTRACT

The El Picacho Tertiary intrusive complex is located in the west-central part of the Sierra de Tamaulipas, in the alkaline province of northeast Mexico. The complex cuts Cretaceous limestone, and it consists of gabbro, kaersutite diorite, syenite, nepheline-rich foidolites (ijolite, urtite, juvite), and trachytic and phonolitic dikes. The nepheline-rich foidolites are affected by alkali metasomatism and contain apatite-rich veins enriched in the rare-earth elements. The nepheline-rich foidolites consist of nepheline (55–91%), pyroxene (4–35%) ($Di_{36}Hd_{39}Ae_{25}$ to $Di_{18}Hd_{37}Ae_{45}$) and orthoclase (0–22%). They are silica-undersaturated rocks (44–50 wt.% SiO_2) with a strongly alkaline character (11–15 wt.% $Na_2O + K_2O$) and low contents of Mg (1–4 wt.% MgO), corresponding to fractionated products of a silica-undersaturated parental magma. The alkaline metasomatism is represented by a slightly peralkaline aegirine fenite, which consists of albite, orthoclase, cancrinite pseudomorphs after nepheline, and Na-pyroxene ($Di_{14}Hd_{27}Ae_{59}$ to $Di_{01}Hd_{27}Ae_{72}$). Mafic-mineral-free fenite also is found in the complex and consists of orthoclase and albite, with minor amounts of interstitial quartz. The apatite-rich veins are composed of radial aggregates of apatite, spherulitic chalcedony, quartz, siderite, calcite, barite, and britholite, which is the main *REE*-mineral in the veins. The total *REE* content in the veins varies from 14600 to 29600 ppm, with strong enrichment in *LREE* (La/Lu ratios range from 308 to 2258). A silicate–carbonate liquid immiscibility model is postulated and discussed in order to explain coherently the petrogenetic relationship of the nepheline-rich foidolites with fenite metasomatism and apatite-rich veins enriched in *LREE*.

Keywords: foidolites, feldspathoidal rocks, *REE* mineralization, alkaline rocks, britholite, carbonatite complexes, Tamaulipas, Mexico.

SOMMAIRE

Le complexe intrusif tertiaire de El Picacho est situé dans le secteur ouest-central de la Sierra de Tamaulipas, et fait partie de la province alcaline du nord-est du Mexique. Le complexe recoupe un calcaire crétacé, et contient des unités de gabbro, diorite kaersutitique, syénite, foïdolites à néphéline (ijolite, urtite, juvite), ainsi que des filons de trachyte et de phonolite. Les foïdolites riches en néphéline sont affectées par une métasomatose alcaline, et contiennent des fis-

sures riches en apatite et enrichies en terres rares. Ces foïdolites contiennent néphéline (55–91%), pyroxène (entre $Di_{36}Hd_{39}Ae_{25}$ et $Di_{18}Hd_{37}Ae_{45}$) (4–35%), et orthoclase (0–22%). Ce sont des roches sous-saturées en silice (44–50% de SiO_2 en poids) qui sont fortement hyperalcalines (11–15% de $Na_2O + K_2O$) et à faibles teneurs en Mg (1–4% MgO), et qui correspondraient à des termes évolués d'une série fractionnée à partir d'un parent aussi sous-saturé. La métasomatose a donné des fénites à aegyrine légèrement hyperalcalines, qui contiennent albite, orthoclase, cancrinite en pseudomorphose de la néphéline, et un pyroxène sodique (entre $Di_{14}Hd_{27}Ae_{59}$ et $Di_1Hd_{27}Ae_{72}$). Nous trouvons aussi des fénites leucocrates, à orthoclase + albite, avec de faibles quantités de quartz, interstitiel. Les fissures riches en apatite contiennent des agrégats fibroradiés d'apatite, chalcédoïne sphérolitique, quartz, sidérite, calcite, barytine et britholite, qui est le porteur principal des terres rares. Les fissures ont une teneur élevée en terres rares, entre 14,600 et 29,600 ppm, et montrent un fort enrichissement en terres rares légères (308 < La/Lu < 2258). Une immiscibilité entre liquides silicaté et carbonaté serait à l'origine des liens pétrogénétiques entre les foïdolites à néphéline, la métasomatose qui a produit les fénites, et les fissures à apatite enrichies en terres rares légères.

(Traduit par la Rédaction)

Mots-clés: foïdolites, roches à feldspathoïdes, minéralisation en terres rares, roches alcalines, britholite, complexes carbonatitiques, Tamaulipas, Mexique.

INTRODUCTION

The northeastern part of Mexico, from the Gulf Coastal Plain near Tampico to the U.S.A. border at the Rio Grande (Fig. 1), is characterized by the presence of several Tertiary alkaline intrusive complexes. They cut Cretaceous limestones, which are gently folded by the Laramide Orogeny. The magmatic suites form part of the alkaline province of eastern Mexico (Demant & Robin 1975, Cantagrel & Robin 1979, Robin 1982), which continues toward the U.S.A. in the Trans-Pecos province of Texas.

The presence of alkaline suites in northeastern Mexico has not been well documented in petro-
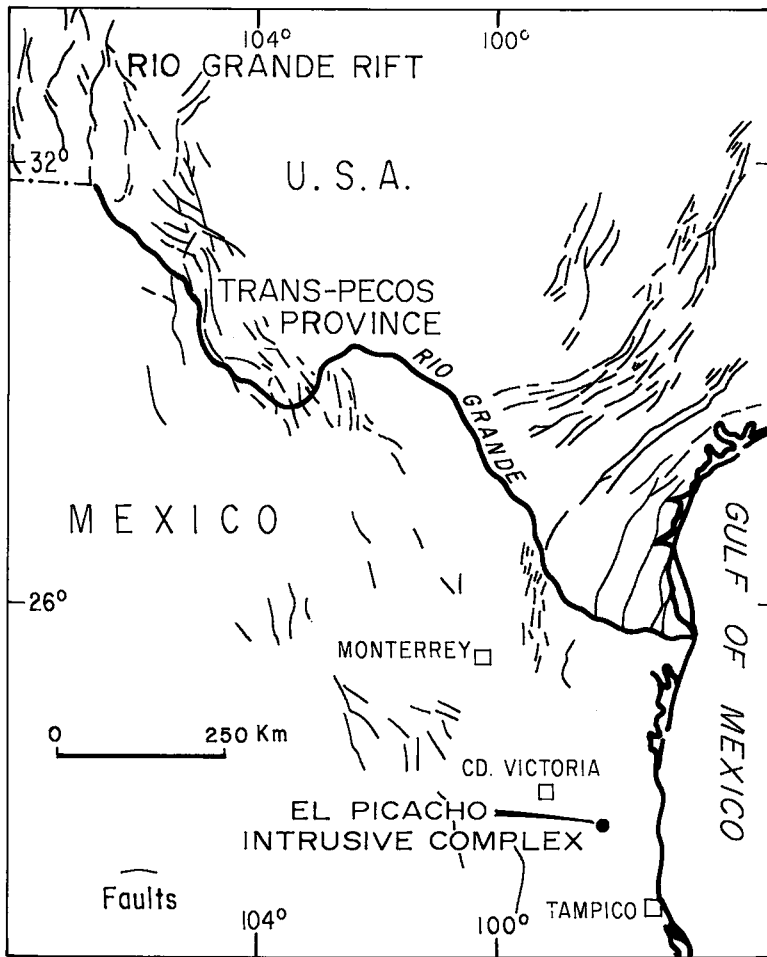
Fig. 1. Location map of the El Picacho intrusive complex. The normal faults are
after King (1969).

graphic, geochemical and geochronological terms; accordingly, their tectonic significance is poorly constrained. For example, few K–Ar ages related to alkaline magmatism at Tamaulipas have been reported: 29.6 ± 1.2 Ma to 27.9 ± 1.1 Ma for syenitic rocks from San Carlos alkaline complex (Bloomfield & Cepeda-Dávila 1973) located 80 km north of Ciudad Victoria, 28.0 ± 0.8 and 23.5 ± 0.7 Ma for a nephelinite volcanic neck and nepheline syenite dome, respectively (Cantagrel & Robin 1979), both hypabyssal alkaline rocks located in the Coastal Plain near Tampico, and 7.0 ± 0.2 Ma for phonolite dikes in the central part of the Sierra de Tamaulipas (Cantagrel & Robin 1979).

The alkaline magmatism is considered by some to be typical of an intracontinental rift zone, without relation to the compressive regime of the Pacific subduction (Cantagrel & Robin 1979, Robin 1982), and

to have been associated with a possible extension of the Rio Grande rift toward the southeast (Bloomfield & Cepeda-Dávila 1973, Robin 1982). However, the Trans-Pecos magmatism, which apparently has an obvious geographic relation to the Rio Grande rift (Fig. 1), is considered to be the far-inland expression of the volcanism produced by the subduction of the Farallon plate along the Pacific coast during the Tertiary (Barker 1979, 1987, Price et al. 1987). This argument is supported by the observed compositional gradation of the Trans-Pecos alkaline magmatism toward the southwest to calc-alkalic magmatism of the Sierra Madre Occidental in western Mexico.

The El Picacho intrusive complex, of alkaline affinity and located approximatly 65 km southeast of Ciudad Victoria in the west-central part of the Sierra de Tamaulipas in northeastern Mexico (Fig.
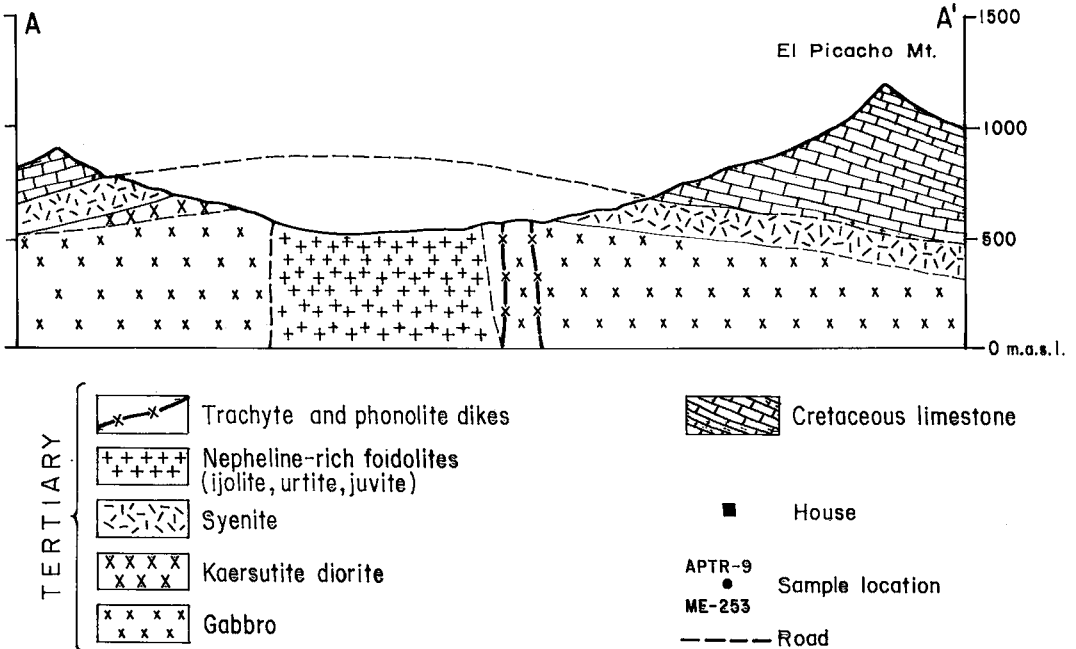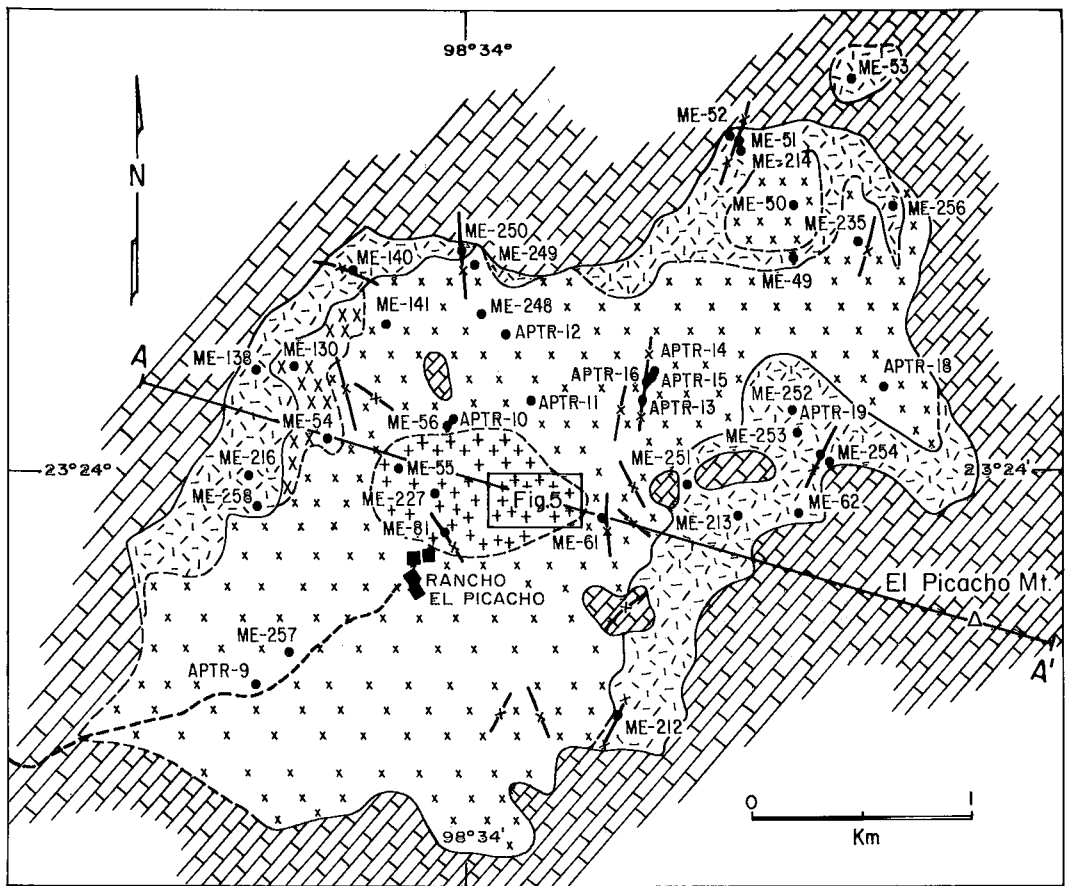
FIG. 2. Simplified geological map of El Picacho intrusive complex and a cross-section through the complex. Inset: area shown in detail in Fig. 5.

1), has never been recognized in the past, and was described as a Tertiary gabbroic intrusive body in unpublished technical reports only. In order to contribute to a better knowledge of this alkaline province, the present paper is devoted to a description of the El Picacho intrusive complex, with emphasis on some peculiar characteristics that make it a unique example known so far in Mexico: presence of nepheline-rich foidolites, fenites, and apatite-rich veins with high contents of the rare-earth elements (*REE*). The complex is exposed in a small ellipsoidal area of about 9 km² (Fig. 2). Its age is unknown, but by extension of the K–Ar data mentioned above, it probably was emplaced in the interval Oligocene to Pliocene.

<div align="center">PETROGRAPHY</div>

Gabbro

The gabbro is the most abundant igneous unit in the El Picacho area (Fig. 2), and the oldest rock in the igneous complex, according to cross-cutting relationships. It is a medium- to coarse-grained mesocratic or melanocratic rock, with a banded structure in some places. The essential minerals are plagioclase (An_{50-70}) and titaniferous augite, with minor amounts of olivine, titaniferous biotite, kaersutite, titaniferous magnetite, ilmenite, apatite and alkali feldspar. The kaersutite, which in some places is abundant (up to 15 vol.%), contains, according to microprobe analyses, around 7.5% TiO_2, and is formed from clinopyroxene. The clinopyroxene and the amphibole are intimately related by means of replacement textures with irregular borders. In areas of banded structure, the texture is of cumulate type, with alternating dark- and light-colored layers rich in clinopyroxene and olivine, and plagioclase, respectively. The thickness of the layers varies from one to several cm.

Kaersutite diorite

The gabbro gradually changes upward into kaer-

sutite diorite. It is observed only in the northwestern part of the El Picacho area (Fig. 2). The kaersutite diorite is a medium-grained mesocratic rock consisting of plagioclase (An_{30-52}), kaersutite, and accessories such as clinopyroxene, olivine, titaniferous biotite, titaniferous magnetite, ilmenite and apatite. The diorite has local variations to banded monzodiorite in which the thin layers (0.5–3 cm) rich in kaersutite alternate with leucocratic layers rich in plagioclase and K-feldspar.

Syenite

Between the gabbro–diorite and the Cretaceous limestone, bodies of leucocratic syenite are found. In some places (ME49, ME256, Fig. 2), the syenite can be seen to cross-cut the gabbro. The contact between the syenite and the limestone is predominantly subhorizontal and parallel to the stratification, and suggests that the syenite bodies are mainly tabular, as is depicted in the cross-section through the complex (Fig. 2).

The leucocratic syenite is a fine- to medium-grained rock with a local coarse-grained miarolitic facies. According to 12 modal analyses and the nomenclature of Streckeisen (1976), the syenite from El Picacho shows a variation from syenite to alkali feldspar syenite and nepheline-bearing alkali feldspar syenite. It is characterized by microperthitic orthoclase (61–96 vol.%). The accessory minerals include plagioclase (An_{7-14}), aegirine–augite, riebeckite, arfvedsonite, nephline and biotite.

Nepheline-rich foidolites

Nepheline-rich foidolites occur in the central part of the complex as a small circular stock (diameter 700–800 m) that cuts the gabbro (Fig. 2). The contact between syenite and foidolites is not observed in the area. ·

The nepheline-rich foidolites are fine- to medium-grained mesocratic rocks with local coarse-grained patches. They consist mainly of nepheline, clinopyroxene and orthoclase (Table 1). The acces-

<div align="center">TABLE 1. MODAL ANALYSES* OF THE NEPHELINE-RICH FOIDOLITES</div>

SAMPLE	IJOLITE					URTITE		JUVITE					
	ME143	ME247	APTR7	SAP10L/D	SAP10AL/D	ME133	ME169	ME61	ME237	ME243	ME244	SAP13L/D	SAP15L/D
Nepheline	55.3	69.8	69.7	64.9	68.6	84.8	91.1	64.8	75.4	70.4	73.5	72.7	62.1
Clinopyroxene	35.2	23.7	20.6	34.2	27.6	11.6	4.6	7.1	7.2	4.0	4.6	6.8	17.9
Orthoclase	0.0	0.0	3.9	0.6	2.9	2.3	2.1	21.1	16.3	21.5	21.8	17.8	15.9
Opaques	6.5	1.0	0.8	0.1	0.1	0.3	0.5	1.8	0.1	0.2	0.0	0.5	1.7
Biotite	0.3	1.2	0.4	0.1	0.3	0.5	0.5	4.3	0.3	1.8	0.0	0.7	0.8
Cancrinite	0.0	0.0	2.5	0.0	0.1	0.0	0.2	0.0	0.1	0.6	0.0	0.8	0.5
Titanite	0.8	3.8	1.3	0.1	0.3	0.1	0.7	0.7	0.3	0.4	0.1	0.5	0.6
Apatite	1.0	0.1	0.2	0.0	0.0	0.4	0.0	0.0	0.1	0.0	0.0	0.0	0.5
Others**	0.9	0.4	0.6	0.0	0.1	0.0	0.3	0.2	0.2	1.1	0.0	0.2	0.0
Total	100.0	100.0	100.0	100.0	100.0	100.0	100.0	100.0	100.0	100.0	100.0	100.0	100.0

* Based on 1000 point counts. ** Include: calcite, zircon, analcite, natrolite.

sory minerals are ilmenorutile, ilmenite, magnetite, biotite, titanite, apatite, zircon, calcite, cancrinite and analcite. These rocks are classified as foidolites in the APF diagram of Streckeisen (1976), but they are classified as ijolite, urtite, or juvite in the MNeA diagram (Fig. 3). The foidolites (ijolite, urtite, juvite) are described as one lithological unit because the compositional variation is local and erratic, and the outcrops are poor.

Although the foidolites have a hypidiomorphic-granular texture (Fig. 4A), parallel arrangement and poikilitic textural variations are common. The fine- to medium-grained variant is rich in pyroxene (Fig. 4B); the medium- to coarse-grained poikilitic variants consist of oikocrysts of nepheline that have inclusions of pyroxene, titanite, ilmenite (Fig. 4C), idiomorphic nepheline and apatite crystals. These textural variations suggest a process of crystal fractionation under varying conditions of pressure and temperature.

The nepheline, present in idiomorphic and hypidiomorphic crystals (Fig. 4A), normally contains small inclusions of acicular pyroxene and apatite. In the coarse-grained material, the feldspathoid is poikilitic (Fig. 4C), and in this case two generations of nepheline are evident; the first occurs in idiomorphic crystals, whereas the second forms allotriomorphic grains that enclose the first.

The orthoclase is present as a late interstitial phase (Fig. 4A). It was identified by its optical properties and X-ray-difraction data. In the juvite, where the feldspar is more abundant, prismatic crystals with Carlsbad twinning are present. In other samples of foidolites, interstitial orthoclase appears between cumulus pyroxene and nepheline grains.

The pyroxene, aegirine–augite, occurs in prismatic and acicular crystals, allotriomorphic intergranular forms, and idiomorphic and hypidiomorphic crystals enclosed by nepheline and orthoclase. Results of electron-microprobe analyses show that the pyroxene in the ijolite samples varies from $Di_{39}Hd_{36}Ae_{25}$ to $Di_{36}Hd_{37}Ae_{27}$ (Table 2); the compositional range in juvite samples is from $Di_{33}Hd_{32}Ae_{35}$ to $Di_{18}Hd_{37}Ae_{45}$ (Table 2; symbols for pyroxene endmembers follow Morimoto 1989). These pyroxene compositional variations suggest that the ijolite and juvite are related through fractional crystallization and could represent fractions of the same batch of magma. The compositional variations coincide with the compositional trends of undersaturated rocks associated with carbonatites (Tyler & King 1967, Mitchell 1980, Le Bas 1987, Andersen 1988).

Aegirine fenite

In several localities (APTR4, APTR5, APTR8, ME142, Fig. 5), medium-grained rocks rich in alkali feldspar have been recognized in small outcrops.
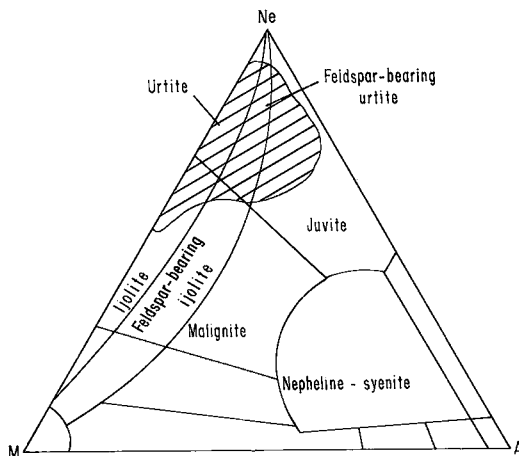

FIG. 3. Mafic minerals – Nepheline – Alkali feldspar (M-Ne-A) triangle showing the range of modal composition of nepheline-rich foidolites (hatchured area), according to Soviet Petrographic Committee (Sørensen 1974, p. 17).

These cut the foidolites by means of a gradual contact characterized by complex replacement textures. These rocks are considered the product of the metasomatic alteration of the foidolites produced by an alkaline aqueous fluid. Unfortunately, the scarcity of exposures in the central part of the area precludes comments concerning the distribution of the fenitized material.

The fenite consists of radial aggregates and trachytic arrangements of hypidiomorphic albite (Fig. 4D), xenomorphic orthoclase, cancrinite pseudomorphs after nepheline, abundant acicular aegirine ($Di_{14}Hd_{27}Ae_{59}$ to $Di_{01}Hd_{27}Ae_{72}$) (Table 2), calcite, and allotriomorphic zircon. The last four minerals are distributed interstitially between albite and orthoclase crystals. Other minor components are strontianite and barite. Calcite and zircon in the fenite are remarkably more abundant than in the foidolites. The pyroxene in this type of fenite is notably depleted in Mg and enriched in Na (Ae_{59-72}) and Fe^{3+} (Table 2), which is consistent with equilibration with a highly alkaline oxygen-rich fluid.

Mafic-mineral-free fenite

In other localities (ME155, ME136), a leucocratic syenitic fenite has been recognized. In this case we also assume a metasomatic origin to account for its complex textural relationships. It consists of allotriomorphic orthoclase and albite with minor amounts of interstitial quartz and chalcedony, accompanied by small grains of britholite, a *REE*-mineral that is radioactive owing to its Th content. Britholite also
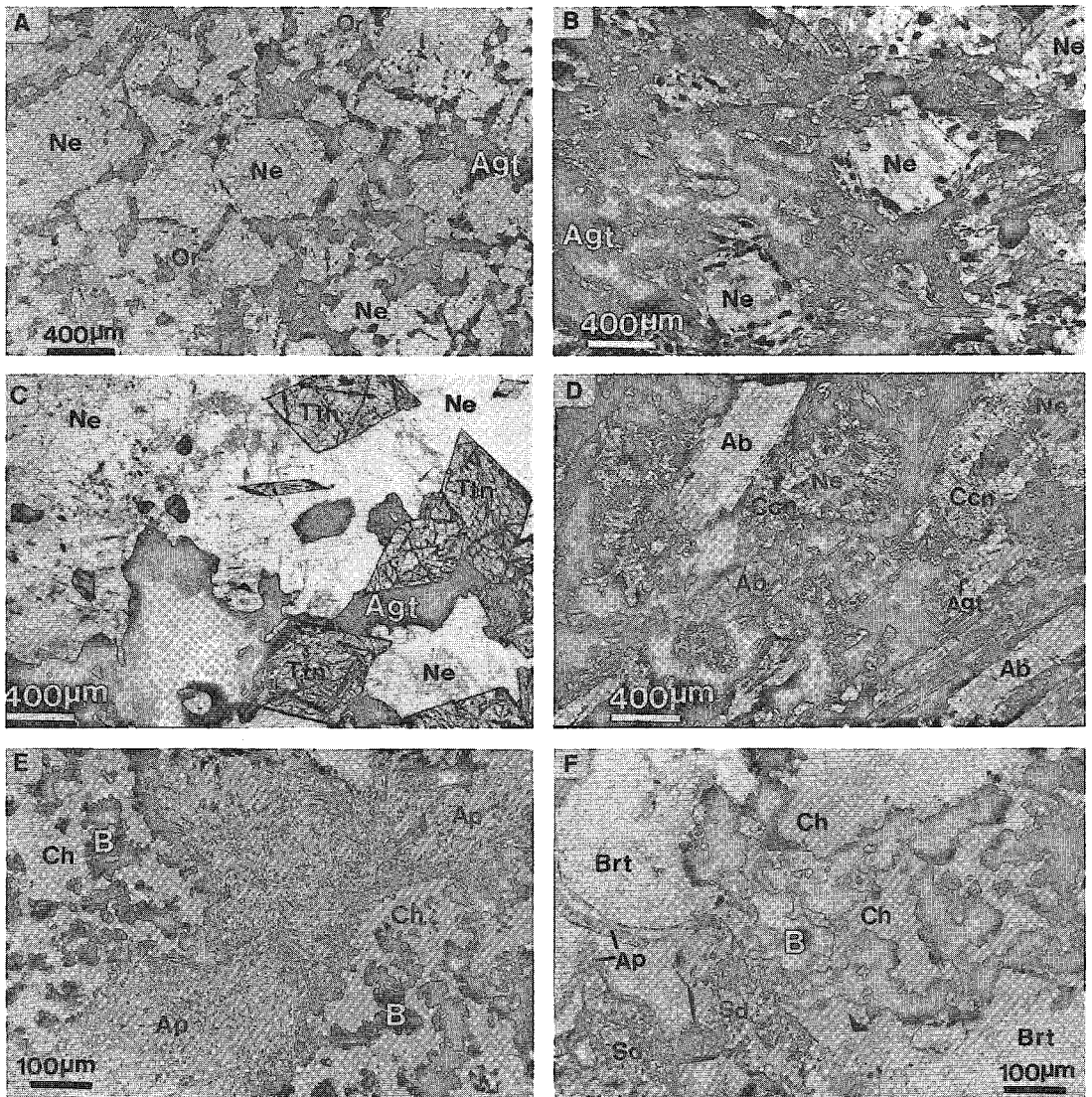
FIG. 4.Photomicrographs of nepheline-rich foidolites, aegirine fenite and apatite-rich veins with *REE* mineralization from El Picacho intrusive complex. A. Feldspar-bearing urtite. Idiomorphic and hypidiomorphic nepheline (Ne) and aegirine–augite (Agt), with minor amounts of interstitial alkali feldspar (orthoclase) (Or), distinguished in the photograph by its dusty appearance. Plane light. B. Ijolite with abundant columnar aegirine–augite (Agt) in parallel arrangement; the matrix is nepheline (Ne). Plane light. C. Ijolite with poikilitic texture, idiomorphic crystals of titanite (Ttn), aegirine–augite (Agt) and opaque enclosed in large crystals of nepheline (Ne). Plane light. D. Aegirine fenite, alkali feldspar (albite) laths (Ab), cancrinite (Ccn) pseudomorphs in corona texture after interstitial nepheline (Ne) and needles of aegirine (Agt). Crossed nicols. E. Apatite-rich vein, radial aggregates of apatite needles, granular aggregates of britholite (B) in matrix of chalcedony (Ch). Plane light. F. Another detail of vein, granular aggregates of britholite (B) in chalcedony (Ch), barite (Brt) and siderite (Sd) crystals surrounded by diminutive apatite crystals (Ap). Plane light.

was identified in the apatite-rich veins, where it is more abundant. The cross-cutting relationships between mafic-mineral-free fenite and the aegirine-

bearing fenite were not observed, but we infer that the leucocratic fenite corresponds to later silica-oversaturated magmatic fluids.

TABLE 2. COMPOSITION OF CLINOPYROXENE FROM IJOLITE, JUVITE AND AEGIRINE FENITE

SAMPLE	IJOLITE		JUVITE		AEGIRINE FENITE				
	SAP10AL/D	SAP10L/D	SAP13L/D	SAP15L/D	APTR4	APTR4	APTR5	APTR5	APTR5
SiO$_2$ wt.%	51.37	51.87	52.99	53.32	55.58	54.74	54.82	54.33	54.71
TiO$_2$	0.54	0.58	0.72	0.59	1.59	3.49	0.41	1.78	0.64
Al$_2$O$_3$	1.27	1.98	1.25	1.16	1.32	1.17	2.24	1.95	1.54
Cr$_2$O$_3$	0.09	0.07	0.03	0.04	0.00	0.03	0.00	0.02	0.02
FeO (total)	17.69	16.32	23.50	18.39	26.01	22.44	29.56	27.95	29.57
MnO	0.57	0.45	0.45	0.55	0.43	0.75	0.09	0.34	0.12
MgO	6.69	7.28	3.47	6.04	1.54	2.75	0.21	0.46	0.16
CaO	16.74	16.68	9.30	13.43	1.49	3.28	0.12	1.25	0.41
Na$_2$O	3.78	3.59	6.37	4.92	9.62	9.20	10.12	9.52	10.33
Total	98.74	98.82	98.08	98.44	97.58	97.85	97.57	97.60	97.50

Structural formulae (4.00 cations, 6.00 oxygen anions):

Si	2.018	2.016	2.110	2.081	2.210	2.150	2.200	2.180	2.209
^{IV}Al	0.00	0.000	0.000	0.000	0.000	0.000	0.000	0.000	0.000
^{VI}Al	0.058	0.090	0.059	0.051	0.061	0.053	0.110	0.092	0.073
Ti	0.015	0.160	0.021	0.017	0.048	0.100	0.010	0.050	0.019
Fe^{3+} *	0.197	0.147	0.391	0.288	0.581	0.447	0.660	0.544	0.698
Fe^{2+}	0.384	0.383	0.391	0.313	0.279	0.290	0.340	0.393	0.299
Mn	0.019	0.014	0.014	0.019	0.014	0.025	0.002	0.012	0.005
Mg	0.392	0.423	0.206	0.352	0.091	0.161	0.002	0.026	0.010
Ca	0.704	0.694	0.397	0.563	0.062	0.138	0.005	0.053	0.017
Na	0.288	0.271	0.493	0.374	0.738	0.701	0.790	0.737	0.810
Cr	0.003	0.002	0.001	0.001	0.000	0.000	0.000	0.001	0.001

Na	26.6	24.8	44.7	35.3	65.8	59.6	69.7	63.1	72.1
Mg	36.2	38.8	18.6	33.3	8.1	13.7	0.2	2.2	0.9
Fe^{2+} + Mn	37.2	36.4	36.7	31.4	26.1	26.7	30.1	34.7	27.0

* Calculated according to Cameron & Papike (1981). The microprobe analyses were done with a JEOL 35-C electron scanning microscope equipped with a Tracor-Northern energy dispersion spectrometer.

Apatite-rich veins (REE mineralization)

Weathered apatite-rich veins are found at the central part of the igneous complex; they are highly radioactive (Fig. 5). Along the Arroyo El Picacho, the width of the veins varies from 0.3 to 3 m (cross-section A–B, Fig. 5). In another locality (ME227, Fig. 2), two more veins were found after trenches were opened; one of these has a width of 4 m. The contact between the veins and nepheline-rich wall-rock is sharp (Fig. 5). The distribution and abundance of the veins are unknown because of the scarcity of exposures. The collection of fresh samples was difficult; however, in various places it was possible to obtain large weathered fragments of vein material from which small and relatively fresh pieces were selected.

The veins consist predominantly of radial aggregates of acicular apatite and interstitial spherulitic chalcedony, with minor amounts of britholite, quartz, siderite and hematite pseudomorphs after pyrite. Other parts of the vein contain allotriomorphic calcite, rhombs of siderite, and minor amounts of spherulitic chalcedony, barite, quartz, apatite, Fe–Ti oxides, and other unidentified constituents. In all chalcedony-rich portions, granular aggregates of britholite crystals are present (Figs. 4E, 4F). The individual crystals vary from several μm up to 50 μm across. Britholite was identified by scanning electron-microprobe analyses and is the principal REE-mineral in the veins. Its ideal formula is

$(Ce,Ca)_5(SiO_4,PO_4)(OH,F)$ (Fleischer 1987), and it is related to the apatite group through the substitution $Si^{4+} + REE^{3+} + Sr + Th \rightleftharpoons P^{5+}Ca^{2+}$ (Ouzegane et al. 1988). The abundance of britholite is around 2%, although it may increase to 10% in the veins.

The textural features in some veins suggest the following paragenetic sequence: pyrite–siderite–calcite–apatite–britholite–barite–chalcedony–quartz. In other cases, the paragenesis is more complex, because different stages of deposition of apatite and britholite are evident during the precipitation of silica.

Britholite is a rare mineral reported in only a few localities worldwide (Winter & Bøggild 1899, Hughson & Sen Gupta 1964, Vlasov 1966, Nash 1972, Ouzegane et al. 1988). The localities are alkaline igneous complexes and carbonatite complexes. In the In'Ouzzal carbonatite complexes, western Ahaggar, Algeria, the apatite–britholite association has been reported in late carbonatites, and britholite is the principal carrier of REE (Ouzegane et al. 1988), as is the case in the El Picacho complex.

Apatite-rich veins and late siliceous veins with REE enrichment similar to those from El Picacho have been described in carbonatite complexes in Malawi (Garson 1966). In the Mountain Pass complex, California, the main REE resource in the world, the LREE are essentially concentrated in veins of late silicified carbonatites in bastnäsite and parisite (Olson et al. 1954). In the Karonge area, Burundi, silica-rich veins with REE mineralization and absence of carbonates are related to a hydrothermal stage of
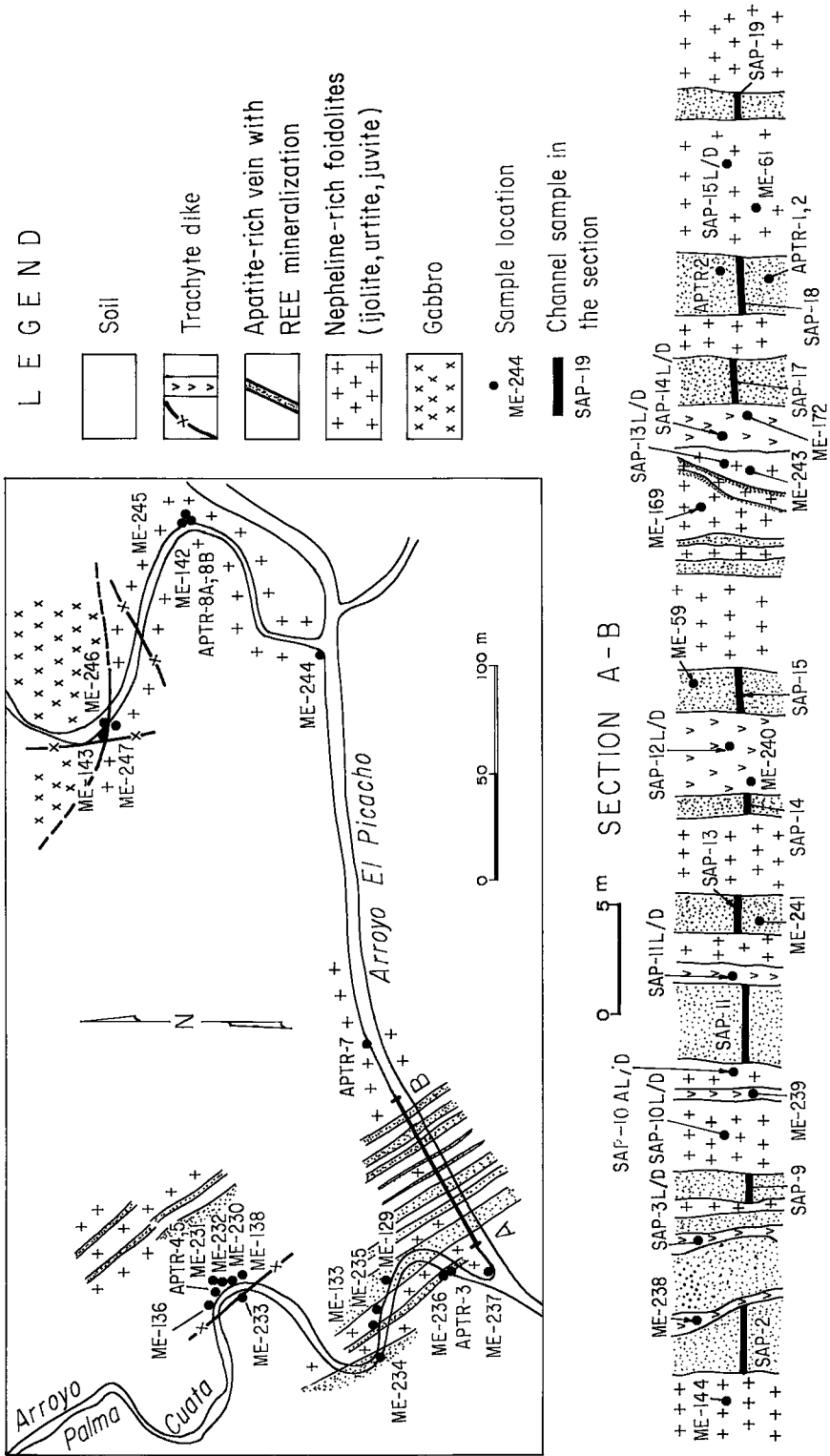
FIG. 5. Geological sketch map of the central part of El Picacho area, and partial cross-section along the Arroyo El Picacho.

TABLE 3. MAJOR AND TRACE ELEMENT CONTENTS OF SELECTED ROCKS FROM EL PICACHO INTRUSIVE COMPLEX

	Gabbro	Nepheline-bearing alkali feldspar syenite		Nepheline-rich foidolite			Aegirine fenite	Apatite rich veins
	APTR9	ME250	ME252	APTR7	SAP10AL/D	SAP13L/D	APTR4	APTR3
SiO_2 wt.%	45.03	57.94	60.41	44.50	46.68	50.19	54.83	42.36
TiO_2	2.07	0.80	0.34	2.86	0.72	0.99	0.32	0.14
Al_2O_3	12.20	19.44	19.02	19.70	17.82	20.37	20.67	1.36
Fe_2O_3	1.90	3.20	2.65	5.15	5.36	4.25	2.40	5.90
FeO	10.15	1.30	1.45	2.74	3.52	1.50	0.50	
MnO	0.18	0.11	0.11	0.14	0.26	0.12	0.13	0.62
MgO	12.81	0.76	0.15	2.34	3.76	0.93	0.16	0.40
CaO	11.74	2.91	1.54	7.40	8.18	3.94	0.66	16.60
Na_2O	1.89	5.17	6.68	11.56	8.90	10.69	11.20	1.76
K_2O	0.47	6.55	5.59	3.05	2.58	4.39	4.10	0.04
P_2O_5	0.45	0.15	0.07	0.30		0.32	0.07	20.96
LOI*	0.08	1.83	1.92	0.15	2.10	2.27	4.39	5.50
Total	98.97	100.16	99.93	99.89	99.86	99.96	99.43	95.64
$Mg/(Mg + Fe^{2+})$ [mol]	0.69	0.51	0.17	0.60	0.65	0.52	0.36	
$Na/(Na + K)$ [mol]	0.86	0.54	0.64	0.85	0.84˙	0.79	0.80	
$(Na + K)/Al$ [mol]	0.29	0.80	0.90	1.13	0.97	1.10	1.10	
Y ppm	<5	14	15	20	<5	14	12	1800
Zr	81	315	550	980	1100	1000	1450	633
Nb	27	125	93	455	165	435	385	160
Rb	6	145	150	90	46	135	96	11
Sr	505	575	225	670	600	960	560	4186
Ba	140	1100	850	1200	400	1400	970	16032
La	15	54.6	67.4	87.4	33	64.6	56.3	4000
Ce	30	100	120	200	66	120	98	5700
Pr	<50	<50	<50	<50	<50	<50	<50	<410
Nd	21	38	36	95	21	45	28	1170
Sm	4.3	6.1	5.9	19.4	6.2	9.2	4.9	522
Eu	2	2	2	5	2	3	1	178
Gd	<200	<200	<200	<200	<200	<200	<200	<1000
Tb	<1	<1	<1	2	<1	1	<1	88
Dy	3	4	4	9	3	6	5	404
Ho	<1	<1	<1	<1	<1	<1	2	59
Er	<100	<100	<100	<100	<100	<100	<100	<480
Tm	<0.5	<0.5	<0.5	<5.8	<1.3	<2	<0.5	<5.2
Yb	0.8	1.8	2.4	2.6	2.6	1.8	2.1	115
Lu	0.2	0.3	0.4	0.5	0.7	0.4	0.4	11.5
Th	1.7	10	21	7.7	6.9	9.3	42	1750
U	<1	<1	4	3	7	2	20	<10
ΣREE**	92	235	257	462	148	273	214	13318
CIPW norms								
or	2.60	39.36	33.00	1.02	14.84	25.78	24.23	
ab	13.05	35.78	50.30		9.26	10.88	32.49	
an	21.92	10.67	5.40		0.97			
ne	1.04	4.72	3.85	44.87	34.69	37.35	27.64	
ac			11.66		8.87	6.95		
lc			13.07					
ns						0.79		
di	25.80	2.53	1.11	14.15	24.68	6.31	2.03	
wo		0.21	7.62	4.40	4.25	0.16		
ol	27.27	2.68						
mt	2.59	2.17	3.85	0.98	7.58	1.69		
il	3.69	1.55	0.65	5.35	1.33	1.83	0.61	
hm				0.35				
ap	0.93	0.36	0.15	0.65		0.70	0.15	

* Loss on ignition. ** For the total REE content from La to Lu, the REE values below detection limits were estimated from the chondrite-normalized pattern. The analyses were commercially carried out in Bondar Clegg Labs., Vancouver, Canada. REE, U and Th were determinated by instrument neutron activation analyses; Y, Zr, Nb, Rb and Sr by X-ray fluorescence analyses; the major element oxides and Ba by plasma emission spectroscopy; FeO by titration; and LOI by gravimetry. The CIPW norm was calculated by means of the GPP commercial program.

TABLE 4. CONCENTRATIONS OF REE AND OTHER TRACE ELEMENTS OF SELECTED CHANNEL
SAMPLES FROM WEATHERED APATITE-RICH VEINS

SAMPLE	SAP2	SAP9	SAP11	SAP13	SAP14	SAP15	SAP17	SAP18	SAP19
Y ppm	2300	840	1100	1600	2000	2200	1400	800	630
La	4000	5000	6000	7000	4000	6000	10000	7000	5000
Ce	6910	7590	8330	9840	6900	9050	12900	10200	6290
Pr	<440	<480	<540	<640	<880	<570	<980	<1200	<880
Nd	1340	1890	1540	1540	1150	1870	1940	2090	1570
Sm	643	609	771	850	642	711	1570	809	464
Eu	280	176	256	283	252	234	477	231	146
Gd	<1000	<1000	<1000	<1000	<1000	<1000	<1000	<1000	<1000
Tb	157	65	102	130	134	122	190	69	54
Dy	277	315	317	446	898	772	278	284	203
Ho	110	16	17	76	91	73	23	15	10
Er	<280	<460	<520	<290	<420	<280	<350	<420	<200
Tm	<6.1	<4.3	<5.9	<6.9	<6.2	<5.7	<8.6	<5.5	<3.9
Yb	120	31	50.2	86.3	117	113	78.4	19	15
Lu	13	2.7	4.7	10	14.8	11.9	5.4	3.1	3.1
Th	2130	1630	2640	3000	2500	2340	2620	2600	1360
U	32	29	30	157	54	33	<22	54	28
ΣREE*	15317	16765	18597	21796	15580	20417	29610	21981	14603

* For the total REE content, the REE values below detection limit were estimated from the chondrite-normalized
pattern. The analyses were commercially carried out in Bondar-Clegg Labs., Vancouver, Canada. REE, Th and
U were determinated by instrument neutron activation analysis; Y by X-ray fluorescence analysis.

carbonatitic differentiation, despite the lack of a direct visible connection with alkaline rocks or carbonatites (Van Wambeke 1977).

Trachyte and phonolite dikes

Dikes of trachyte and phonolite cross-cut all previously described rocks, so that they are the last magmatic event. Their thickness varies from 20–30 cm to several meters. The trachyte consists of phenocrysts of Na-plagioclase, alkali feldspar, and kaersutite in a trachytic matrix. The phonolite dikes contain phenocrysts of nepheline, alkali feldspar and aegirine–augite, with a groundmass rich in acicular greenish pyroxene with a tinguaitic texture. Although the age of trachyte and phonolite dikes in the area is unknown, they may be correlated with phonolite dikes in the central part of the Sierra de Tamaulipas, 25 km SE of El Picacho, from which one K–Ar date of 7.0 ± 0.2 Ma has been reported (Cantagrel & Robin 1979).

GEOCHEMISTRY

Major and trace elements

Table 3 shows the composition of selected rocks from the El Picacho complex, and Table 4 displays the Y, REE, Th and U contents in selected channel samples from apatite-rich veins. The corresponding REE patterns are illustrated in Figure 6, and the abundances of the incompatible trace elements normalized to a primordial mantle are shown in Figure 7.

Although total alkalis versus silica plots of several samples of gabbro are ambiguous, it does have an alkaline affinity because it contains normative ne (Table 3); according to the mineralogical criteria of Wilkinson (1974), it can be classified as an alkaline mafic rock by the presence of titaniferous augite, kaersutite, labradorite and alkali feldspar. The distribution of trace elements in the gabbro, however, is different from that in the other alkaline rocks of the complex (Figs. 6, 7). The REE content (92 ppm) and their fractionation (La/Lu = 75) in the gabbro are within the range for alkaline olivine basalts, according to the data compiled by Cullers & Graf (1984). It has the lowest REE content and La/Lu ratio of any rocks in the complex. The ratio Eu/Sm, 0.46, is slightly high, and is the expression of a small positive Eu anomaly (Fig. 6), which reflects the abundance of plagioclase. The apparent negative Yb anomaly is probably an analytical feature. On the other hand, the gabbro shows a relative depletion in Rb, K and Zr (Fig. 7), which could be attributed to refractory minor phases, such as phlogopite and zircon, during a partial melting in the mantle. The slight enrichment in Nb, Sr and P is probably related to Ti-bearing minerals and apatite.

The nepheline-rich foidolites are silica-undersaturated rocks, with peralkaline variations [(Na + K)/Al > 1, molar basis], which have abundant normative ne and ac (Table 3). The high Na/(Na + K) ratio, in the range 0.79–0.85, indicates the strongly sodic nature of these rocks. The REE contents in the foidolites are slightly higher than those in the nepheline-bearing alkali feldspar syenites. Their REE distribution is similar, except in foidolite SAP10AL/D, whose REE content is low (148 ppm) and whose fractionation is different (Fig. 6). The foidolite sample SAP10AL/D was collected 30 cm away from one of the apatite-rich veins, and

probably was affected by late hydrothermal fluids related to the veins. The *REE* patterns of foidolites and syenites (Fig. 6) do not show any Eu anomaly, which suggests that plagioclase was not an important residual solid phase after partial melting or fractional crystallization.

The *REE* content, and principally the *LREE*, in the nepheline-rich foidolites from the El Picacho complex is several times lower than the *REE* enrichment in similar rocks from Canadian carbonatite complexes (*e.g.*, Eby 1975, Cullers & Medaris 1977) and Soviet alkaline complexes (Gerasimovsky 1974). The *LREE* content in the foidolites, nevertheless, is similar to the *LREE* average of melanephelinites from African complexes (Le Bas 1987).

On the other hand, the foidolites from El Picacho show a marked enrichment in Nb and Zr, probably related to titanite and zircon (Fig. 7). The foidolites and syenite are depleted in Sr and P, indicating fractionation of apatite in their genesis. The syenites show depletion in Nb and Ti in relation to the foidolites, probably due to precipitation of titanite. The Zr/Ti ratio in both types of rocks is high; this ratio appears to be a sensitive index of fractionation (Le Bas 1987).

The aegirine fenite is characterized by enrichment in silica and alkalis, and depletion in Fe, Mg, and Ca in relation to nepheline-rich foidolites. This chemical feature is correlated with increased alkali feldspar and depletion of mafic minerals in the fenite. The LOI, 4.39 wt.%, is assumed to reflect the content of $CO_2 + H_2O^+$, related predominantly to considerable amounts of cancrinite. The fenite is sodic [$Na/(Na + K) = 0.8$], slightly peralkaline, with normative *ac* and *ns*. Its chemical composition is similar to that of agpaitic nepheline syenites. The *HREE* distribution in this fenite is seemingly irregular, with an apparently positive Ho anomaly (Fig. 6); however, it is probable that the latter is due to an analytical problem. In any case, the *HREE* contents are presumably related to zircon, and so is the strong enrichment in Th, U, Nb and Zr (Fig. 7). The aegirine fenite shows relative depletion in Rb, K, *LREE*, P and Ti, which reflects the absence of K-feldspar, apatite and Ti-bearing minerals.

The *REE* content in a fresh apatite-rich vein sample (APTR3) is 13300 ppm (Table 3). In weathered samples, the content varies from 14600 to 29600 ppm (Table 4). A preliminary examination of the *REE* distribution in the veins suggests a *LREE* enrichment, with *HREE* depletion in the weathered samples with respect to the fresh sample (Fig. 6). However, the variation of *REE* content in the weathered and unweathered samples is more likely related to the abundance of britholite and apatite than to the influence of weathering. The distribution of both minerals in the veins is variable, so that the *REE* content in APTR3 is a long way from being a represen-
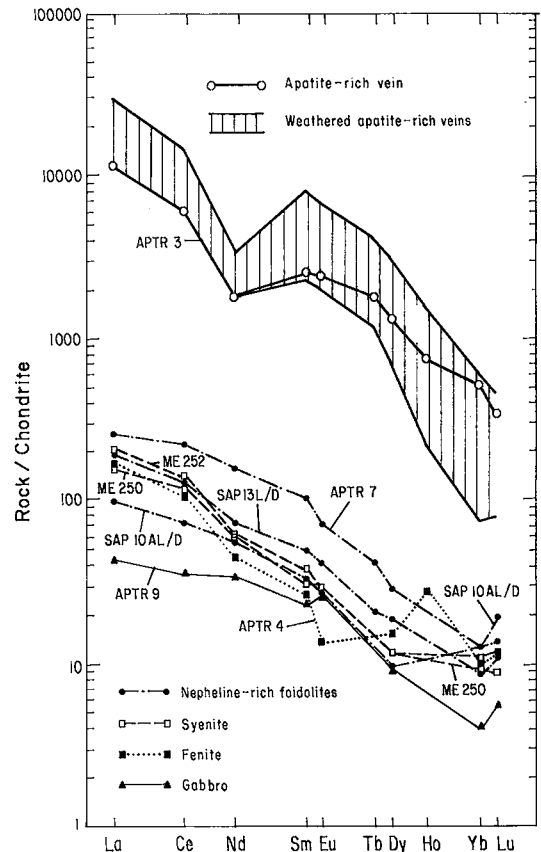

FIG. 6. Chondrite-normalized *REE* patterns for gabbro (solid triangle), syenite (open squares), nepheline-rich foidolites (solid circles), aegirine fenite (solid square), apatite-rich vein (open circle) and range of *REE* content defined by nine channel samples of weathered apatite-rich veins (hatchured area). The values used in normalization are from Haskin *et al.* (1968).

tative value of the fresh veins, and it is not a good reference point for an accurate evaluation of the *REE* mobility under the weathering effects. For comparative purposes, we consider that the influence of weathering on the total *REE* contents in the veins is negligible.

The strong *LREE* enrichment in the apatite-rich veins (La/Lu ratio varies from 308 to 2258) is similar to that in carbonatites (*e.g.*, Loubet *et al.* 1972, Eby 1975, Mitchell & Brunfelt 1975, Cullers & Medaris 1977, Möller *et al.* 1980, Woolley & Kempe 1989). The range of the total *REE* content in the veins (13300–29600 ppm) is greater than the range in the majority of the carbonatites (72–15515 ppm) (Cullers & Graf 1984), and similar to that in ferrocarbonatite (Woolley & Kempe 1989). The *REE* enrich-
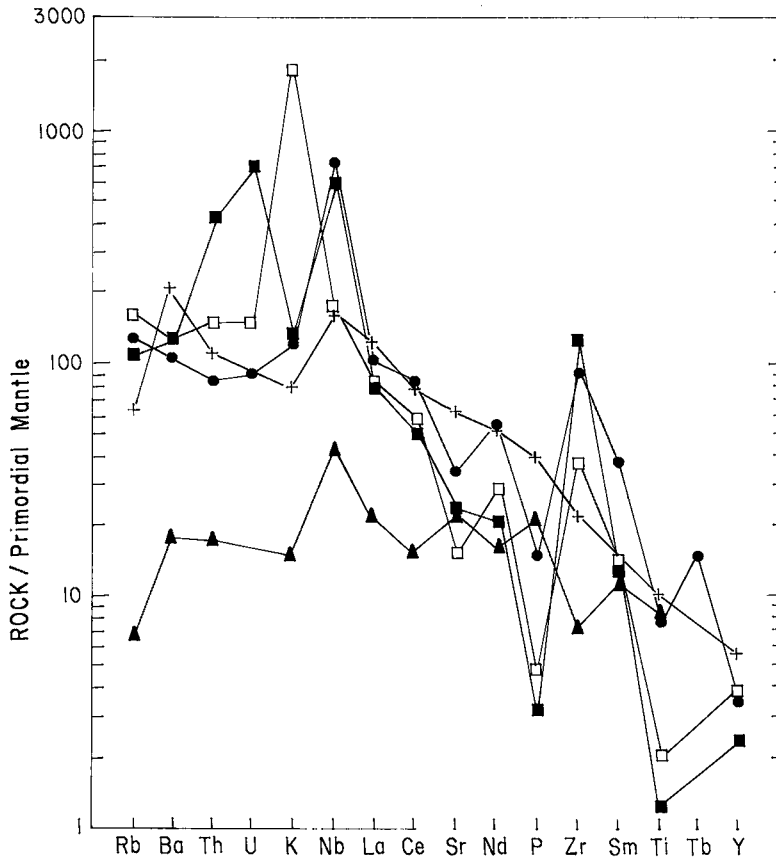
FIG. 7. Plots of incompatible element abundances normalized to primordial mantle (Wood 1979) for gabbro (solid triangle), averaged values of two samples (ME250, ME252) of syenite (open square), average values of two samples (APTR7, SAP13L/D) of nepheline-rich foidolites (solid circle), and aegirine fenite (solid square) from El Picacho intrusive complex. The average trace-element abundances of melanephelinites from Tertiary carbonatite complexes in eastern Africa are shown for comparison (Le Bas 1987) (cross). The elements are arranged in order of increasing bulk partition-coefficient for mantle mineralogies (Wood 1979).

ment in the veins is several tens of times higher than the *REE* content in the nepheline-rich wallrock (Fig. 6). This ratio, veins/foidolites, is unusually higher than the carbonatite/ijolite ratio found in different carbonatite complexes, which ranges from one to ten (Cullers & Graf 1984, Fig. 7.3).

The *REE* fractionation in the veins is characterized by an average Sm/Nd ratio of 0.47. This value is abnormal in comparison to all igneous rocks, in which the Sm/Nd ratio varies from 0.11 to 0.32 (Faure 1986, p. 201). The high Sm/Nd ratio in the veins implies important Nd depletion (Fig. 6), incompatible with the increase in degree of differentiation. A reasonable way to explain this feature is to postulate a hydrothermal mineralogical zoning, with

precipitation at depth of other *REE* minerals, such as aeschynite-(Nd) or rhabdophane-(Nd), which are common in *REE* mineralization *via* hydrothermal processes (Vlasov 1966). On the other hand, the Nd depletion may reflect an analytical problem related with the INAA method (R. L. Cullers, pers. comm.).

Another important enrichment in the veins in relation to the wallrocks of nepheline-rich foidolite occurs with Ba, Th, Sr, P and Y (Table 3). There is depletion in Rb, Nb and Zr. These geochemical features, in addition to the strong enrichment in *LREE*, are typical of late carbonatites (Kapustin 1971, 1983, Barber 1974, Le Bas 1981, 1987) or carbonatites formed hydrothermally (Borodin & Kapustin 1968).

DISCUSSION

In the present state of knowledge of the El Picacho area, it is difficult to constrain a petrogenetic evaluation of the complex. However, we can discuss some petrogenetic aspects that will provide a useful working hypothesis for further work in the complex.

The gabbro–diorite relationship is best understood. The banded structure with cumulate textures in both rocks and the gradual contact imply a gravity fractionation in a magma chamber in which the successive residual liquids became enriched in alkalis and volatile components, giving rise to a dioritic composition rich in amphibole in the upper part of the chamber. The banded kaersutite monzodiorite may represent the most differentiated product from the gabbroic magma.

On the other hand, the field observation and the petrographic and geochemical data suggest that the gabbro–diorite is not comagmatic with the syenite and foidolites. In terms of *REE* contents, the gabbro can be reasonably explained by 19% partial melting of mantle with a peridotite source containing 25% olivine, 51.2% orthopyroxene, 20% clinopyroxene, and 3.8% garnet (Fig. 8A). In this quantitative model, the initial *REE* contents of the garnet lherzolite are those suggested by Frey *et al.* (1978) for an enriched and fractionated mantle related to the generation of alkaline mafic rocks, with the *LREE* 7–9 times and the *HREE* 2.5–3 times chondrite values. The equation for equilibrium melting and crystallization described by Haskin (1984) and *REE* partition coefficients reported by Frey *et al.* (1978) in their set 1 were used for this model. The $Mg/(Mg + Fe^{2+})$ ratios for several nonbanded samples of gabbro vary from 0.69 to 0.79, and correspond to those expected for primary melts from the mantle (Roeder & Emslie 1970, Frey *et al.* 1978, Wilkinson 1982), and they are consistent with the model.

We contend that gabbro and the foidolites could not be derived from the same peridotite source by variable degrees of partial melting. The best model involves 3–4% partial melting, but the predicted *HREE* differ from those of the foidolites (Fig. 8A). The *REE* contents of foidolites can be explained by 3% partial melting of the same enriched mantle, but with a different lherzolite source, consisting of 41.5% olivine, 40% clinopyroxene, 17% orthopyroxene, and 1.5% garnet. The $Mg/(Mg + Fe^{2+})$ ratios of the foidolites (Table 3) and some petrographic features suggest a magma modified by fractional crystalliza-
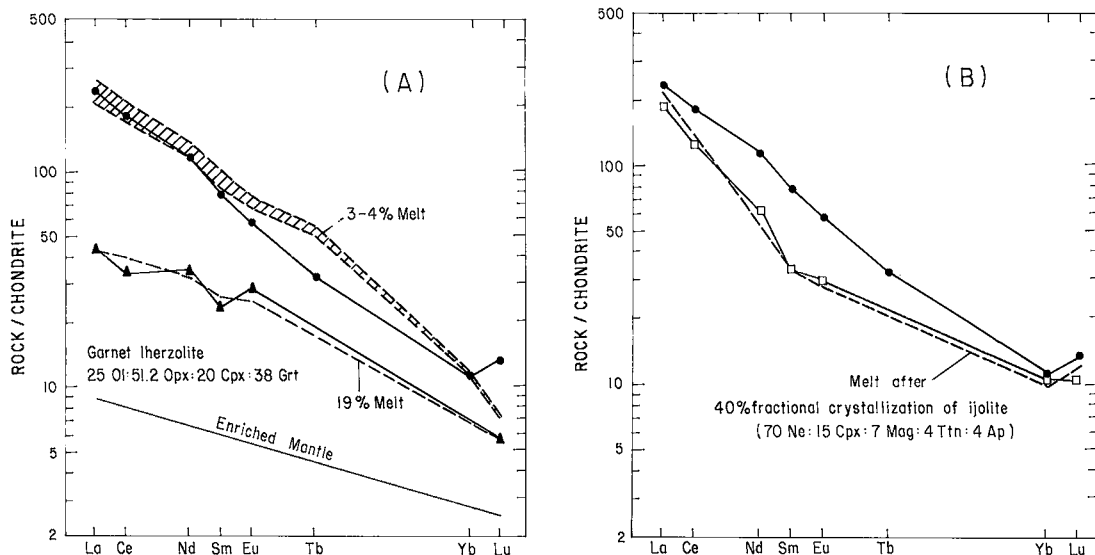

FIG. 8. A. Models of partial melting for the generation of the various mantle-derived melts from enriched garnet lherzolite mantle (Frey *et al.* 1978). Gabbro (solid triangle), averaged values of two samples (APTR7, SAP13L/D) of foidolites (solid circle). Predicted *REE* content of the melt with the ratio of the 25 olivine:51.2 orthopyroxene:20 clinopyroxene:3.8 garnet in the peridotite source; 19% melting (dashed line); the dashed diagonally ruled field represents various degrees of partial melting from 3% (top of field) to 4% (bottom of field). B. Fractional crystallization model. Averaged value of two samples (ME250, ME252) of syenite (open square), foidolites (solid circle). The dashed line represents a melt after 40% fractional crystallization of an ijolite in the ratio of 70 nepheline:15 clinopyroxene:7 magnetite:4 titanite: 4 apatite, fairly similar to some modal analyses of the foidolites, and similar in *REE* to the foidolites.

tion or other processes rather than a primary melt. It is probable that at least two parental magmas were involved at certain times during the evolution of the complex.

The gabbro cannot be related with the foidolites and syenite by fractional crystallization; all proportions of modal compositions of gabbro crystallizing at any percentage produce residual melts with a different *REE* distribution from that of foidolites and syenite. On the other hand, if minerals in the ratio fairly similar to some modal analyses of ijolite (Table 1), 70% nepheline, 15% clinopyroxene, 7% magnetite, 4% titanite, and 4% apatite, precipitate from an initial melt having a *REE* content the same as the foidolites, the predicted *REE* content of the residual melt is similar to that of the syenite after 40% crystallization (Fig. 8B). Cumulate textures in rocks rich in nepheline and aegirine–augite in the foidolites are in accord with this process. The important depletion in Sr, P and Ti in the syenite (Fig. 7) also is consistent with a fractional crystallization model from this type of ijolitic magma. Thus, a comagmatic relationship between foidolites and syenite is suggested by their trace-element signatures. The equation for fractional crystallization with continuous removal of crystals described by Haskin (1984) and the partition coefficients for nepheline, clinopyroxene, magnetite, and titanite reported by Cullers & Medaris (1977), and apatite (Nagasawa 1970) were used.

The nepheline-rich foidolites, according to their petrographic and geochemical characteristics, may correspond to fractionated products from a silica-undersaturated parental magma, probably a single primary carbonated nephelinitic magma (*e.g.*, Middlemost 1974, Rock 1976, Le Bas 1987). The low Mg content, the high alkali content, the abundance of Ti–Cr-poor clinopyroxene, and the absence of mantle-type xenoliths in the foidolites are features similar to melanephelinites; although such nephelinites are commonly associated with carbonatites, presumably by liquid immiscibility (Le Bas 1987, 1989), no carbonatite body has been recognized in the area. The blocks of limestone surrounded by igneous rocks (Fig. 2) were converted to marble that retained its stratification, with banded structures rich in garnet and epidote; such marble can easily be distinguished from carbonatite. Although the foidolites do not show calcite-rich ocellar textures that may be interpreted as relics of immiscible magmas (*e.g.*, Ferguson & Currie 1971, Philpotts 1976, 1982, Bogoch & Magaritz 1983, Treiman & Essene 1985), they contain minor amounts of interstitial calcite, which indicates a certain primary CO_2 content in this magma and, in some cases, is interpreted as residual carbonate remaining dissolved in the silicate melt after the immiscible separation of the carbonate melt (Le Bas 1987). Also the composition of the foidolites is similar to experimental immiscible liquids KH42 and KH27 of Kjarsgaard & Hamilton (1988), and with liquid FH24 of Freestone & Hamilton (1980) (Fig. 9). In the first case, the immiscibility occurs at 5 kbar
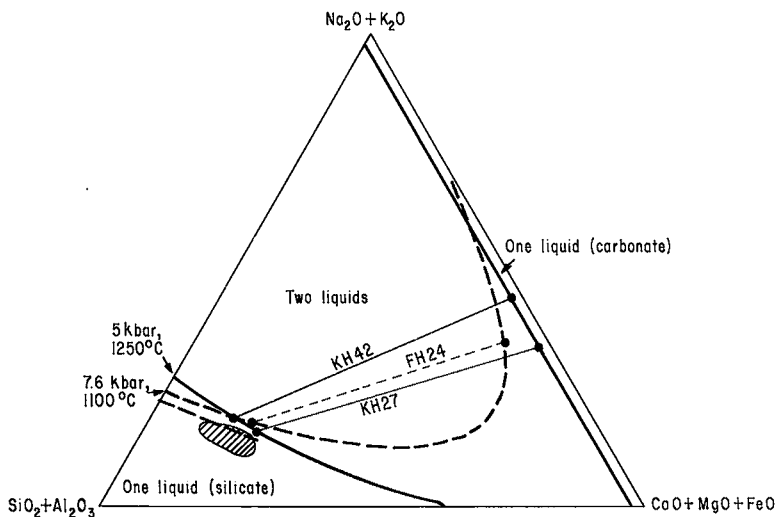

FIG. 9. Location of compositional range (wt.%) of the nepheline-rich foidolites (hatchured area) on the 5 kbar silicate-carbonate liquid solvus diagram of Kjarsgaard & Hamilton (1988), including tie-lines KH42 and KH27. The 7.6 kbar solvus of Freestone & Hamilton (1980) also is shown (dashed line), including their tielines FH24. The short dashed line in the lower-left corner is the estimated *circa* 15 kbar solvus (Le Bas 1989). See text for discussion.

and 1250°C, whereas in the second, it occurs at 7.6 kbar and 1100°C. The corresponding immiscible carbonate liquids are rich in alkalis, Fe and Mg (Fig. 9). Moreover, the nepheline-rich foidolites abut the solvus defining the two-liquid field at around 15 kbar (Le Bas 1989) on the liquid immiscibility diagram (Fig. 9). Thus, the chemical composition of the foidolites shows good agreement with experimental results, and a possible immiscible carbonate melt is suggested. We cannot exclude the existence of a carbonatite body at depth.

Silicate–carbonate liquid immiscibility is considered to be an important process in the genesis of carbonatite, as is indicated by numerous experimental studies (Koster van Groos & Wyllie 1966, 1968, 1973, Watkinson & Wyllie 1971, Freestone & Hamilton 1980, Kjarsgaard & Hamilton 1988, 1989). Furthermore, various authors have proposed this magmatic process to explain the high *REE* content in carbonatite bodies in relation to comagmatic alkaline rocks (Eby 1975, Mitchell & Brunfelt 1975, Cullers & Medaris 1977). It also could explain the strong *REE* enrichment in the apatite-rich vein from El Picacho complex. This enrichment cannot be explained by simple hydrothermal remobilization from the nepheline-rich foidolites to the veins. The foidolites do not show hydrothermal alteration that could support an intense migration of fluids, and they do not have unusually strong *REE* depletion that could have been directly related with the strong *REE* enrichment in the adjacent veins. Therefore, the genetic association between wallrock and veins, if any, is not simple. The carbonate-bearing apatite-rich veins, although they are not carbonatites according to the nomenclature of Streckeisen (1979) and Woolley & Kempe (1989), may represent a hydrothermal stage of a carbonatite magma, as is suggested by their trace-element contents. Their mineralogy, characterized by the lack of silicates, is more consistent with a hydrothermal than a magmatic origin.

In the liquid immiscibility model, the fenitization could be due to the loss of alkalis from carbonate immiscible melt, according to the hypothesis that an alkali-rich carbonatite magma fractionated at decreasing temperature, lost alkalis and became enriched in incompatible elements (Le Bas 1981, 1987, Woolley 1982). Experimental studies at temperatures above 750°C involving two immiscible liquids, a silica-undersaturated peralkaline silicate liquid and a carbonate liquid rich in Ca, have proved the existence of a fluid. This phase is an aqueous vapor rich in Na, SiO_2 and CO_2 (Koster van Groos & Wyllie 1968, 1973), which is consistent with various chemical features of aegirine fenite (Table 3), in which the abundance of cancrinite and calcite suggests a high CO_2 content (essentially equivalent to LOI). Although we do not have sufficient data to characterize the fenites from the El Picacho complex,

their mineralogical variation could be reasonably interpreted as compositional evolution of fenitizing fluids during the thermal decrease according to the model of Rubie & Gunter (1983).

The peralkaline aegirine fenite, rich in albite, sodic pyroxene (Ae_{59-72}) and nepheline, may result from sodic metasomatism formed by high-temperature residual fluids, whereas the mafic-mineral-free fenite, constituted by orthoclase, albite, and minor amounts of interstitial quartz (ME55, ME136), may represent a late, low-temperature stage of K-fenitization.

The presence of quartz, chalcedony and britholite in the low-temperature late potassic fenite suggests a genetic relationship between this fenite and the veins. The apatite-rich veins cannot be interpreted as a residual stage of the fenitizing fluids, owing to the absence of silicate and alkalis. However, if the fenites are considered to arise from the loss of alkalis from a possible carbonate immiscible melt, which gradually became enriched in silica and incompatible elements, and if the veins represent the later residual (hydrothermal) stage of this melt, both types of rocks, fenites and veins, must have been derived from the same volatile-rich magma, although they represent different degrees or stages of differentiation.

CONCLUSIONS

The El Picacho Tertiary intrusive complex has several petrographic and geochemical characteristics that suggest the presence of a carbonatite complex. They are as follows: 1) Silica-undersaturated alkaline rocks such as nepheline-rich foidolites (ijolite, urtite, juvite) are typical alkaline rocks associated with carbonatite (Tuttle & Gittins 1966, Heinrich 1966, Eby 1975, Cullers & Medaris 1977, Le Bas 1981, 1987). 2) Fenite metasomatism is another common phenomenon in carbonatite complexes, although the fenites in the El Picacho area apparently occur in small amounts only. 3) Apatite-rich veins and late siliceous veins with *REE* enrichment similar to those from El Picacho have been described in carbonatite complexes only. 4) The strong enrichment in *LREE*, Sr, Ba and Th in the apatite-rich veins from El Picacho is characteristic of late carbonatites (Borodin & Kapustin 1968, Kapustin 1971, 1983, Barber 1974, Le Bas 1981, 1987).

There are, however, some points that argue against a carbonatite affinity for El Picacho: 1) In the Tertiary alkaline province, from the Gulf Coastal Plain in Mexico to the Trans-Pecos area of Texas, carbonatite rocks have not been found, and the region does not have features of an epeirogenic uplift or a continental rift, which are "normal" environments of carbonatite occurrences. Nonetheless, carbonatites occur also in other types of environment, including oceanic regions (Le Bas 1984). 2) There is no car-

bonatite exposed in the El Picacho area, although the outcrops are not abundant. We cannot exclude the existence of carbonatite beneath the present level of exposure of the complex.

Of course, this hypothesis needs to be tested with more geochemical data, especially isotopic and chronological data, in order to constrain the consanguinity of the different rocks of the complex and sources.

REFERENCES

ANDERSEN, T. (1988): Evolution of peralkaline calcite carbonatite magma in the Fen Complex, southeast Norway. *Lithos* **22**, 99-112.

BARBER, C. (1974): The geochemistry of carbonatites and related rocks from two carbonatites complexes, south Nyanza, Kenya. *Lithos* **7**, 53-63.

BARKER, D. S. (1979): Cenozoic magmatism in the Trans-Pecos province; relation to the Rio Grande Rift. *In* Rio Grande Rift; Tectonics and Magmatism (R.E. Riecker, ed.). *Am. Geophys. Union*, 382-392.

———— (1987): Tertiary alkaline magmatism in Trans-Pecos Texas. *In* Alkaline Igneous Rocks (J.G. Fitton & B.G.J. Upton, eds.). *Geol. Soc. London, Spec. Publ.* **30**, 415-431.

BLOOMFIELD, K. & CEPEDA-DÁVILA, L. (1973): Oligocene alkaline igneous activity in NE Mexico. *Geol. Mag.* **110**, 551-555.

BOGOCH, R. & MAGARITZ, M. (1983): Immiscible silicate–carbonate liquids as evidenced from ocellar diabase dykes, southeast Sinai. *Contrib. Mineral. Petrol.* **83**, 227-230.

BORODIN, L. S. & KAPUSTIN, YU. L. (1968): Genetic types of rare-element deposits. *In* Geochemistry and Mineralogy of Rare Elements and Genetic Types of their Deposits III (K.A. Vlasov, ed.). Israel Program for Scientific Translations, Jerusalem, Israel.

CAMERON, M. & PAPIKE, J.J. (1981): Structural and chemical variations in pyroxenes. *Am. Mineral.* **66**, 1-50.

CANTAGREL, J.-M. & ROBIN, C. (1979): K–Ar dating on eastern Mexican volcanic rocks – relations between the andesitic and the alkaline provinces. *J. Volc. Geotherm. Res.* **5**, 99-114.

CULLERS, R. L. & GRAF, J. L. (1984): Rare earth elements in igneous rocks of the continental crust; predominantly basic and ultrabasic rocks. *In* Rare Earth Element Geochemistry (P. Henderson, ed.). Elsevier, Amsterdam (237-274).

———— & MEDARIS, L.G. (1977): Rare earth elements in carbonatite and cogenetic alkaline rocks: examples from Seabrook Lake and Callander Bay, Ontario. *Contrib. Mineral. Petrol.* **65**, 143-153.

DEMANT, A. & ROBIN, C. (1975): Las fases del volcanismo en México; una síntesis en relación con la evolución geodinámica desde el Cretácico. *Univ. Nal. Autón. México, Inst. Geología, Revista* **1**, 70-83.

EBY, G.N. (1975): Abundance and distribution of the rare-earth elements and yttrium in the rocks and minerals of the Oka carbonatite complex, Quebec. *Geochim. Cosmochim. Acta* **39**, 597-620.

FAURE, G. (1986): *Principles of Isotope Geology* (2nd edition). John Wiley & Sons, New York.

FERGUSON, J. & CURRIE, K.L. (1971): Evidence of liquid immiscibility in alkaline ultrabasic dikes at Callander Bay, Ontario. *J. Petrol.* **12**, 561-585.

FLEISCHER, M. (1987): *Glossary of Mineral Species* (5th edition). The Mineralogical Record, Tucson, Arizona.

FREESTONE, I.C. & HAMILTON, D.L. (1980): The role of liquid immiscibility in the genesis of carbonatites – an experimental study. *Contrib. Mineral. Petrol.* **73**, 105-117.

FREY, F.A., GREEN, D.H. & ROY, S.D. (1978): Integrated models of basalt petrogenesis: a study of quartz tholeiites to olivine melilitites from southeastern Australia utilizing geochemical and experimental petrological data. *J. Petrol.* **19**, 463-513.

GARSON, M.S. (1966): Carbonatites in Malawi. *In* Carbonatites (O.F. Tuttle & J. Gittins, eds.). John Wiley & Sons, New York (33-71).

GERASIMOVSKY, V.I. (1974): Trace elements in selected groups of alkaline rocks. *In* The Alkaline Rocks (H. Sørensen, ed.). John Wiley & Sons, London (402-412).

HASKIN, L.A. (1984): Petrogenetic modelling - use of rare-earth elements. *In* Rare Earth Elements

Geochemistry (P. Henderson, ed.). Elsevier, Amsterdam (115-152).

_____, HASKIN, M.A., FREY, F.A. & WILDEMAN, T.R. (1968): Relative and absolute terrestrial abundances of the rare-earths. *In* Origin and Distribution of the Elements (L.H. Ahrens, ed.). Pergamon Press, Oxford, England (889-912).

HEINRICH, E. W. (1966): *The Geology of Carbonatites.* Rand McNally & Co., Chicago, Illinois.

HUGHSON, M.R. & SEN GUPTA, J.G. (1964): A thorium intermediate member of the britholite apatite series. *Am. Mineral.* **49**, 937-951.

KAPUSTIN, YU. L. (1971): Mineralogy of Carbonatites. Published for the Smithsonian Institution and the National Science Foundation, Washington, D. C., Amerind Publishing, New Delhi, 1980.

_____ (1983): Strontium and barium geochemistry in carbonatite complexes. *Geochem. Int.* **20**(4), 1-14.

KING, P.B. (1969): Tectonic map of North America scale 1:5,000,000. U. S. Geol. Surv., Reston Va.

KJARSGAARD, B. A. & HAMILTON, D. L. (1988): Liquid immiscibility and the origin of alkali-poor carbonatites. *Mineral. Mag.* **52**, 43-55.

_____ & _____ (1989): The genesis of carbonatite by immiscibility. *In* Carbonatite Genesis and Evolution (K. Bell, ed.). Unwin Hyman, London (388-404).

KOSTER VAN GROOS, A.F. & WYLLIE, P.J. (1966): Liquid immiscibility in the system Na_2O-Al_2O_3-SiO_2-CO_2 at pressures to 1 kilobar. *Am. J. Sci.* **264**, 234-255.

_____ & _____ (1968): Liquid immiscibility in the join $NaAlSi_3O_8$-Na_2CO_3-H_2O and its bearing on the genesis of carbonatites. *Am. J. Sci.* **266**, 932-967.

_____ & _____ (1973): Liquid immiscibility in the join $NaAlSi_3O_8$-$CaAl_2Si_2O_8$-Na_2CO_3-H_2O. *Am. J. Sci.* **273**, 465-487.

LE BAS, M. J. (1981): Carbonatite magmas. *Mineral. Mag.* **44**, 133-140.

_____ (1984): Oceanic carbonatites. *In* Kimberlites and Related Rocks (J. Kornprobst, ed.). Elsevier, Amsterdam (169-178).

_____ (1987): Nephelinites and carbonatites. *In* Alkaline Igneous Rocks (J.G. Fitton & B.G.J. Upton, eds.), *Geol. Soc. London, Spec. Publ.* **30**, 53-83.

_____ (1989): Diversification of carbonatite. *In* Carbonatite Genesis and Evolution (K. Bell, ed.). Unwin Hyman, London (428-447).

LOUBET, M., BERNAT, M., JAVOY, M. & ALLÈGRE, C.J.

(1972): Rare-earth contents in carbonatites. *Earth Planet. Sci. Lett.* **14**, 226-232.

MIDDLEMOST, E. A. K. (1974): Petrogenetic model for the origin of carbonatites. *Lithos* **7**, 275-278.

MITCHELL, R. H. (1980): Pyroxenes of the Fen alkaline complex, Norway. *Am. Mineral.* **65**, 45-54.

_____ & BRUNFELT, A.O. (1975): Rare earth geochemistry of the Fen alkaline complex, Norway. *Contrib. Mineral. Petrol.* **52**, 247-259.

MÖLLER, P., MORTEANI, G. & SCHLEY, F. (1980): Discussion of *REE* distribution patterns of carbonatites and alkalic rocks. *Lithos,* **13**, 171-179.

MORIMOTO, N. (1989): Nomenclature of pyroxenes. *Can. Mineral.* **27**, 143-156.

NAGASAWA, H. (1970): Rare earth concentrations in zircons and apatites and their host dacite and granites. *Earth Planet. Sci. Lett.* **9**, 359-364.

NASH, W.P. (1972): Apatite chemistry and phosphorus fugacity in a differentiated igneous intrusion. *Am. Mineral.* **57**, 877-886.

OLSON, J.C., SHAWE, D.R., PRAY, L.C. & SHARP, W.N. (1954): Rare-earth mineral deposits of the Mountain Pass district, San Bernardino County, California. *U.S. Geol. Surv., Prof. Pap.* **261**.

OUZEGANE K., FOURCADE, S., KIENAST, J.R. & JAVOY, M. (1988): New carbonatite complexes in the Archaean In'Ouzzal nucleus (Ahaggar, Algeria): mineralogical and geochemical data. *Contrib. Mineral. Petrol.* **98**, 277-292.

PHILPOTTS, A.R. (1976): Silicate liquid immiscibility: its probable extent and petrogenetic significance. *Am. J. Sci.* **276**, 1147-1177.

_____ (1982): Compositions of immiscible liquids in volcanic rocks. *Contrib. Mineral. Petrol.* **80**, 201-218.

PRICE, J.G., HENRY, C.D., BARKER, D.S. & PARKER, D.F. (1987): Alkalic rocks of contrasting tectonic settings in Trans-Pecos Texas. *In* Mantle Metasomatism and Alkaline Magmatism (E.M. Morris & J.D. Pasteris, eds.). *Geol. Soc. Am., Spec. Pap.* **215**, 335-346.

ROBIN, C. (1982): Relations volcanologie-magmatologie-géodynamique: application au passage entre volcanismes alcalin et andésitique dans le sud mexicain. *Annales Scientifiques de l'Université de Clermont-Ferrand II. Géologie Minéralogie,* **70**.

ROCK, N.M.S. (1976): The role of CO_2 in alkali rocks genesis. *Geol. Mag.* **113**, 97-113.

ROEDER, P.L. & EMSLIE, R.F. (1970) Olivine–liquid equilibrium. *Contrib. Mineral. Petrol.* **29**, 275-289.

Rubie, D.C. & Gunter, W.D. (1983): The role of speciation in alkaline igneous fluids during fenite metasomatism. *Contrib. Mineral. Petrol.* **82**, 165-175.

Sørensen, H. (ed.) (1974): *The Alkaline Rocks.* John Wiley & Sons, London.

Streckeisen, A. (1976): To each plutonic rock its proper name. *Earth-Sci. Rev.* **12**, 1-33.

_____ (1979): Classification and nomenclature of volcanic rocks, lamprophyres, carbonatites and melilitic rocks: recommendations and suggestions of the IUGS Subcommission on the Systematics of Igneous Rocks. *Geology* **7**, 331-335.

Treiman, A.H. & Essene, E.J. (1985): The Oka carbonatite complex, Quebec: geology and evidence for silicate–carbonate liquid immiscibility. *Am. Mineral.* **70**, 1101-1113.

Tuttle, O.F. & Gittins, J., eds. (1966): *Carbonatites.* John Wiley & Sons, New York.

Tyler, R.C. & King, B.C. (1967): The pyroxenes of the alkaline igneous complexes of eastern Uganda. *Mineral. Mag.* **36**, 5-21.

Van Wambeke, L. (1977): The Karonge rare earth deposits, Republic of Burundi: new mineralogical-geochemical data and origin of the mineralization. *Miner. Deposita* **12**, 373-380.

Vlasov, K.A. (1966): *Geochemistry and Mineralogy of Rare Elements and Genetic Types of their Deposits.* I. Israel Program for Scientific Translations, Jerusalem, Israel.

Watkinson, D.H. & Wyllie, P.J. (1971): Experimental study of the composition join $NaAlSiO_4$–$CaCO_3$–H_2O and the genesis of alkalic rock-carbonatite complexes. *J. Petrol.* **12**, 357-378.

Wilkinson, J.F.G. (1974): The mineralogy and petrography of alkali basaltic rocks. *In* The Alkaline Rocks (H. Sørensen, ed.). John Wiley & Sons, New York (67-95).

_____ (1982): The genesis of mid-ocean ridge basalt. *Earth-Sci. Rev.* **18**, 1-57.

Winter, C. & Bøggild, O.B. (1899): On some minerals from the nepheline syenite at Julianehaab, Greenland (epistolite, britholite, shizolite and steenstrupite). *Medd. om Grønland* **24**, 190-196.

Wood, D.A. (1979): A variably veined suboceanic upper mantle – genetic significance for mid-oceanic ridge basalts from geochemical evidence. *Geology* **7**, 499-503.

Woolley, A.R. (1982): A discussion of carbonatite evolution and nomenclature, and the generation of sodic and potassic fenites. *Mineral. Mag.* **46**, 13-17.

_____ & Kempe, D.R.C. (1989): Carbonatite: nomenclature, average chemical compositions, and element distribution. *In* Carbonatite Genesis and Evolution (K. Bell, ed.). Unwin Hyman, London (1-14).